Ultrafast investigation and control of Dirac and Weyl semimetals

Chris P. Weber[1, a)]

Department of Physics, Santa Clara University, 500 El Camino Real, Santa Clara, CA 95053-0315, USA

(Dated: 4 January 2021)

Ultrafast experiments, using sub-picosecond pulses of light, are poised to play an important role in the study and use of topological materials, and particularly of the three-dimensional Dirac and Weyl semimetals. Many of these materials' characteristic properties—their linear band dispersion, Berry curvature, near-vanishing density of states at the Fermi energy, and sensitivity to crystalline and time-reversal symmetries—are closely related to their sub- and few-picosecond response to light. Ultrafast measurements offer the opportunity to explore excitonic instabilities and transient photocurrents, the latter depending on the Berry curvature and possibly quantized by fundamental constants. Optical pulses may, through Floquet effects, controllably and reversibly move, split, merge, or gap the materials' Dirac and Weyl nodes; coherent phonons launched by an ultrafast pulse offer alternate mechanisms for similar control of the nodal structure. This Perspective will briefly summarize the state of research on the ultrafast properties of Dirac and Weyl semimetals, emphasizing important open questions. It will describe the challenges confronting each of these experimental opportunities, and suggest what research is needed for ultrafast pulses to achieve their potential of controlling and illuminating the physics of Dirac and Weyl semimetals.

I. INTRODUCTION

Recent years have seen a blossoming of research on topological, three-dimensional (3D) materials whose low-energy quasiparticles are Dirac or Weyl fermions, and whose bands disperse linearly and cross massless at a node. The achievement of Dirac and Weyl semimetals in real materials (for instance Cd_3As_2 and TaAs, respectively) allows the investigation of new fundamental physics. These materials could also be technologically useful: their mobility,[1] thermopower,[2] magnetoresistance,[1] and spin-Hall angle[3] are usually large. They could be ingredients in a quantum amplifier or a chiral battery,[4] or targets for the detection of sub-MeV dark matter.[5] This Perspective will explore the ways that ultrafast experiments can advance the study and utility of 3D Dirac and Weyl semimetals.

Since these materials have been ably reviewed elsewhere,[2,6,7] including in this Special Topic (*Editors, please insert citations*), a brief introduction will suffice. A Weyl point is characterized by an electronic dispersion that is linear in three dimensions—upper and lower cones meeting at a node, Fig. 1a, when visualized as energy *vs.* two dimensions of momentum—and by a definite chirality, *i.e.* a spin that remains either parallel or antiparallel to the electrons' velocity. A Weyl point may also be thought of as a monopole of Berry curvature, so that the total Berry flux through a momentum- ($\vec{k}$-) space surface containing a single Weyl point is quantized.

When opposite-chirality Weyl points meet in $\vec{k}$-space, they can annihilate, opening a gap at the node,[8,9] or they can overlap without gapping to form a Dirac point, which is spin-degenerate and therefore lacks chirality (Fig. 1b). Variations on the Dirac and Weyl theme include nodal-line semimetals (with a continuous line of Dirac nodes)

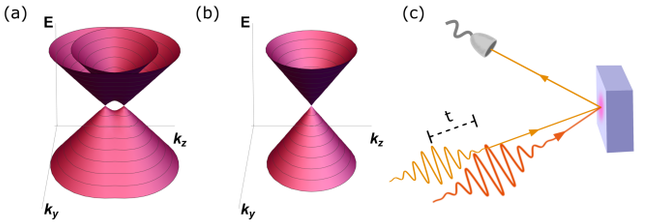

FIG. 1. Schematic electron dispersions of **(a)** a Weyl semimetal, with a pair of opposite-chirality nodes, or **(b)** a Dirac semimetal, with a single non-chiral node. **(c)** The principle of a pump-probe reflectivity experiment. The probe, arriving a time t after the pump, is reflected and detected.

such as ZrSiS,[10] type-II Weyl semimetals (whose Weyl cones are tilted to form pockets of electrons and holes) such as T_d-WTe_2,[11] multifold semimetals (with threefold or higher band degeneracy at the node) such as RhSi,[12] and magnetic Weyl semimetals[13,14] such as $Co_3Sn_2S_2$ and Mn_3Sn. The physics particular to each of these classes of material will typically manifest only if the Fermi energy, E_F, lies close to a node.

Dirac and Weyl semimetals are both sensitive to crystal symmetries, but in opposite ways. For the crossing of two bands to form a stable Dirac point—one that will not be gapped by small changes in the Hamiltonian, *i.e.* that is not "fine-tuned"—requires that the crystal preserve certain symmetries.[15] Weyl semimetals, in contrast, are not required to preserve any particular symmetry, but they must *break* either time-reversal or inversion symmetry. Though time-reversal is typically broken by an external magnetic field or by a material's spontaneous magnetization, a strong, short pulse of circularly-polarized light may serve the same purpose, briefly splitting a Dirac point into two Weyl points.[8,9] That light can potentially alter these materials so profoundly suggests the importance of studying their optical, and particularly their ul-

a)Electronic mail: cweber@scu.edu

trafast optical, properties.

Most optical measurements probe states in a material's bulk, making the Dirac and Weyl fermions in 3D materials more amenable to optics than those in graphene or on the surfaces of topological insulators. Indeed, the materials' intrinsic interest and their potential for optical and optoelectronic uses are enhanced by many exotic optical properties, predicted or observed. Their optical conductivity is linear in frequency, or constant for nodal-line materials,[16] and may include step functions tunable by external fields.[17] They exhibit partially spin-polarized photocurrent driven by circularly-polarized mid-IR light (Sec. III) and anisotropic photoconductivity,[18] while films should exhibit resonant transparency at THz frequencies tuned by a magnetic field[19] and a mid-IR passband lying between E_F and $2E_F$.[20]

A material's ultrafast dynamics refers to its sub- and few-picosecond response to excitation by an optical pulse, and is measured using "pump" and "probe" pulses, both typically of $20 - 100$ fs duration (Fig. 1c). Upon interaction with the pump, the sample's properties are briefly changed, principally by excitation of electrons and phonons and by modification of the electronic band structure. The changes can be monitored with a probe pulse arriving a variable time (of order picoseconds) after the pump—for instance by measuring the reflectivity, transmissivity, or photoelectron spectrum. As the sample relaxes toward equilibrium, the measured property returns to its pre-excitation value. Ultrafast experiments are useful for observing materials perturbed far from equilibrium, for resolving very fast processes, and for rapidly controlling materials' optical and electronic properties.

The ultrafast responses of several Dirac and Weyl semimetals have been measured and are already being put to practical use: the materials have been used to make a passive optical switch for picosecond mode-locking of a mid-infrared laser[21] and broadband infrared photodetectors[22,23] whose response time can be just a few picoseconds. Photocurrent in Weyl semimetals has an intrinsic lifetime below a picosecond and flows without applied bias, pointing the way to fast, low-noise mid-infrared detectors.[23] Dirac semimetals have proven efficient in generating high harmonics in the terahertz range,[24] and Weyl semimetals are expected to show strong four-wave mixing.[25]

Further knowledge of these materials' response to photoexcitation will be important for basic research—in realizing a predicted exciton condensate,[26] relating photocurrents to electronic topology, or achieving proposed effects in which intense pulses of light might separate or merge pairs of Weyl points,[8,9,27,28] open or close gaps at Dirac points,[9,29] or convert nodal lines to point nodes.[28,30] This Perspective will start by discussing what can be learned from the ultrafast properties themselves, the progress that has been made and the important open questions (Sec. II), then explore the ways in which ultrafast measurements can help accomplish some even more exciting goals, such as the quantized injection of photocurrent (Sec. III) and the possibility of controlling Dirac and Weyl materials on ultrafast timescales (Sec. IV).

II. ULTRAFAST THERMODYNAMICS

Many ultrafast experiments on Dirac and Weyl semimetals have focused on photocarrier dynamics: the rates and mechanisms by which photoexcited electrons and holes relax to their initial states. The questions such research asks are essentially thermodynamic ones: Which states are occupied, and which unoccupied? Is the occupation function described by a Fermi-Dirac distribution, and of what temperature? How quickly, and by what means, does heat pass from electrons to phonons? Ultrafast excitation, by driving a material far from equilibrium, can explore these thermodynamic questions under otherwise inaccessible conditions.

For Dirac and Weyl semimetals, answering these questions is valuable for several reasons. The first is practical: photocarriers relax much like the hot electrons important in high-field devices.[31] These processes also dictate the performance of optoelectronic devices. For instance, the several-picosecond response times of a Cd_3As_2 photodetector[23] and optical switch[21] closely match the few-picosecond rate at which its electrons cool.[32–36] Second is the new physics to be learned: the photocarrier dynamics of Dirac and Weyl semimetals differ in interesting ways from those of metals and semiconductors—the paradigmatic materials of ultrafast dynamics—as well as from graphene and topological insulators,[37] the semimetals' two closest analogs. Finally, as I will detail below, understanding these materials' ultrafast thermodynamics can contribute critically toward some of the field's most ambitious goals: exploring exciton insulators, linking the nonlinear optical response to topological invariants, and modifying band topology controllably, reversibly, and literally in a flash.

A. The pump and the probe

The first step in an ultrafast experiment is the excitation of the sample by a short optical "pump" pulse. Intraband (Drude) absorption of the pulse heats the electron gas, while interband absorption creates excess electrons and holes in a non-thermal distribution.

The pump often consists of 1.5-eV (800-nm) photons. This is the energy of a Ti:Sapphire laser, but is not ideally suited to studying the ultrafast properties of Dirac or Weyl fermions: for most materials 1.5-eV optical transitions are available to or from non-Dirac bands,[38] and 1.5 eV often exceeds the range of the bands' linear dispersion, so the pump can excite *non*-Dirac electrons and holes. Some of these carriers quickly relax into the Dirac cone, as shown by ultrafast ARPES,[39–41] but others relax without passing through the Dirac or Weyl bands—likely the majority, considering the low density of states

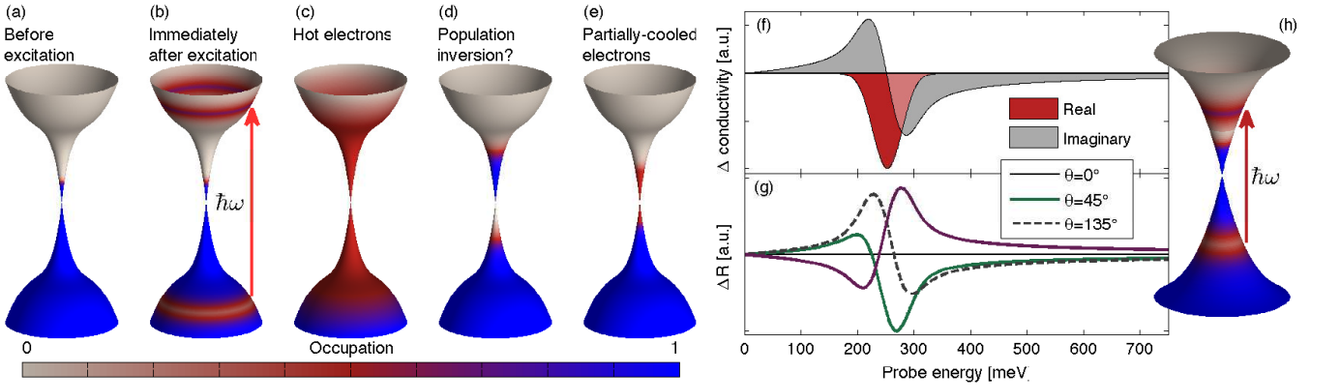

FIG. 2. **(a)-(e)**: Schematic representation of the excitation and relaxation of electrons and holes in a Dirac or Weyl semimetal. Time runs left to right. The many non-Dirac bands far from the Fermi energy are represented by broad continuua above and below the node. The material is shown slightly n-type. **(h)**: Mid-infrared excitation may produce purely Dirac (or Weyl) electrons and holes. **(f)** and **(g)** $\Delta\sigma$ and ΔR *vs.* ω_{probe} are shown for phase-space filling in a narrow energy range, such as panels (b) or (h). θ in panel (g) is the argument of the material's complex conductivity σ, evaluated at ω_{probe}.

near a Dirac point. It is preferable to use a mid-infrared pump pulse, which excites Dirac carriers directly and exclusively, but few experiments have done so.[33,42,43]

The most widely-used measure of a material's ultrafast response is the change in its reflectivity, $\Delta R(t)$. Years of ultrafast studies of semiconductors have identified four principal mechanisms by which photoexcitation may contribute to ΔR,[44–46] and all four occur in Dirac and Weyl semimetals. The first is the pump's excitation of, and the probe's coupling to, a coherent phonon; this phenomenon, recognizable by oscillations in $\Delta R(t)$, is discussed in Section IV B.

Second, photoexcitation may alter the Drude conductivity of free carriers by changing the carrier density N, the scattering time τ, or the the high-frequency dielectric constant ϵ_∞. Reflectivity cannot distinguish changes in N from those in ϵ_∞, since they appear in the optical conductivity only through the screened plasma frequency $\omega_p^{\text{scr}} = \sqrt{4\pi Ne^2/(m\epsilon_\infty)}$. However, if the probe is broadband, and particularly if it spans frequencies near ω_p^{scr}, fits to $\Delta R(\omega)$ can distinguish changes in τ from those in ω_p^{scr}. For instance, Kirby *et al.*[47] showed that excitation of the nodal-line semimetals ZrSiS and ZrSiSe caused a sub-picosecond decrease in ω_p^{scr}, which they attributed to an increase in electronic screening and ϵ_∞. For $t > 1$ ps, ω_p^{scr} recovered while τ was reduced, likely by heating.

The third contribution to ΔR is band renormalization (called "band-gap renormalization" in semiconductors), in which excited carriers modify the electronic dispersion. Optical reflectivity has not shown this effect in Dirac or Weyl semimetals, but ARPES has.[39,41] In ZrSiSe, photoexcitation reduces the group (band) velocity of surface states near E_F. Ordinarily the low density of states near a node results in weak screening of the Coulomb interaction and strong correlations. Consistent with Ref. 47, Gatti *et al.*[41] attribute the modified dispersion to additional screening by excited carriers.

Fourth, and often dominant, is phase-space filling (PSF), in which the occupation of a state above the node by an electron (or below the node by a hole) suppresses further optical absorption *via* the Pauli exclusion principle. The connection between this suppressed absorption and ΔR is made in three steps, detailed pedagogically in the supplement to Ref. 42 and illustrated in Fig. 2f-g: PSF changes the real part, σ_1, of the optical conductivity, with $\Delta\sigma_1 < 0$; the Kramers-Kronig relations prescribe a corresponding change in the imaginary part, σ_2; and ΔR is a function of both σ and $\Delta\sigma$. For Dirac and Weyl semimetals, good approximations are available that make all three steps tractable,[42] particularly if the PSF occurs only for states within the Dirac or Weyl cone—which may be ensured by using an appropriately low pump energy.

Note that even when phase-space is filled only for transitions at a single frequency (Fig. 2f,g), the Kramers-Kronig relations require nonzero $\Delta\sigma_2$ and ΔR over a wide range of frequencies. Thus, though the probe measures ΔR at a single frequency, it is not energy-specific, despite occasional assertions to the contrary; $\Delta R(\omega_{\text{probe}})$ is influenced by optical transitions at many frequencies (Fig. 2g; see Eq. S5 of Ref. 42 or Eq. 14 of Ref. 44). Ultrafast ARPES or core-level spectroscopy[48] allow greater energetic specificity. To a lesser degree, so do optical probes that measure the complex optical response, such as heterodyne-detected transient-grating spectroscopy[32] and time-domain THz spectroscopy.[35] In these experiments the sign of $\Delta\sigma_2$ may constrain whether $\Delta\sigma_1$ occurs at energies above or below the probe (Fig. 2f).

B. Time-dependence

Figure 2a-e illustrates the sequence of events occurring after photoexcitation. Immediately upon photoexcitation (Fig. 2b), PSF causes $\Delta\sigma_1 < 0$ right at the pump frequency ω_{pump}, while $\Delta\sigma_2$ is nonzero over a broader range of frequencies, and ΔR may be positive or nega-

tive depending on both $\sigma(\omega_{\text{probe}})$ and on whether ω_{probe} lies below or above ω_{pump} (Fig. 2f-g). This phenomenon is consistent with a short "spike" in $\Delta R(t)$ seen in many pump-probe experiments: the spike is prominent in degenerate experiments[32,33,49–51] ($\omega_{\text{pump}} = \omega_{\text{probe}}$), and often small[42] or absent[33,34] in non-degenerate ones. The spike is brief because carriers soon scatter into different states and cease to fill phase-space for transitions at ω_{pump}. Their scattering contributes to *thermalization*, the process by which the non-thermal distribution of electrons of Fig. 2b evolves into a hot Fermi-Dirac distribution (Fig. 2c).[33,42,50] At this point a two-temperature model (TTM), with a carrier temperature T_e higher than that of the lattice, may be apt. I will argue, however, that the TTM is most interesting when it is violated.

A spike in $\Delta R(t)$ may alternately arise from very rapid electronic cooling[32,49,52]—if thermalization proceeds too rapidly to resolve, if the timescales of cooling and thermalization overlap, or if the thermalization of photoexcited electrons with background electrons serves to cool the former and heat the latter. Finally, if the spike's duration equals the cross-correlation of the pump and the probe, it may arise from one of several effects commonly called the "coherent artifact,"[53] some of which may be diagnosed or mitigated by changing the beams' relative polarizations.

The dominant processes after thermalization are *cooling* and *recombination* of electrons and holes. The two are intimately related, because if E_F lies close to the node, the electron and hole populations are strong functions of T_e (Figs. 3a,c). The effect is stronger than in semiconductors, where the population remains weakly dependent on temperature until T_e is comparable to the donor or acceptor energy. (On the other hand, if E_F lies far from the node, the semimetal resembles a metal: a thermalized distribution has only a single type of carrier, whose population is independent of T_e, as in Figs. 3b,d. Recombination, then, must occur during thermalization, prior to cooling.)

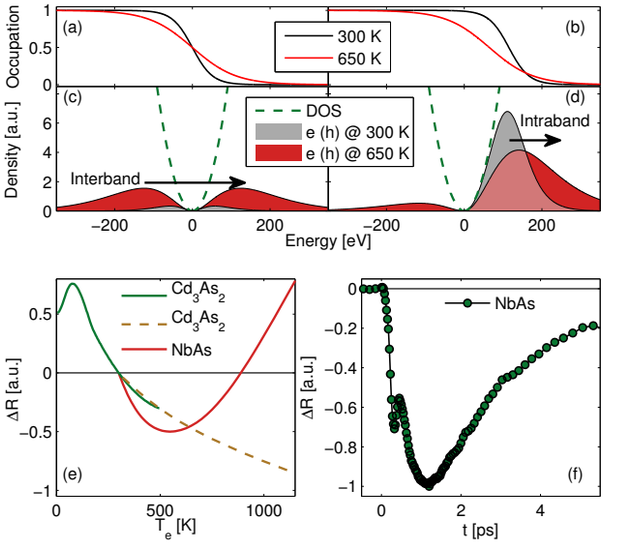

FIG. 3. **(a,b)** Fermi-Dirac distributions at room temperature and 650 K for Dirac semimetals with (a) $E_F = 0$ and (b) $E_F = 115$ meV. **(c,d)** Electron and hole density (and density of states), for the same two cases. Heating a semimetal with a high E_F does little to increase the carrier density. **(e)** Modeled $\Delta R(T_e)$, referenced to 300 K, for Cd_3As_2 (probe 310 meV) and NbAs (270 meV). **(f)** $\Delta R(t)$ for NbAs measured at room temperature with mid-infrared pump and 270-meV probe, showing the "spike" feature and a non-monotonic transient consistent with monotonic cooling. Data in (e) from Refs. 34, 36, and 42, and in (f) from 42; used with permission.

1. Population inversion and the exciton insulator

If cooling outpaces recombination—if there exist times fast compared to recombination but slow compared to cooling—the TTM is not valid. Electrons and holes will accumulate near the node, with distinct Fermi-Dirac distributions and distinct chemical potentials (Fig. 2d). The resulting population inversion could potentially support broad-bandwidth lasing in poorly-served regions of the mid-infrared. Better yet, the vanishing density of states at a node promotes many-body instabilities, making optically pumped Dirac and Weyl semimetals potentially suitable for studying the elusive exciton insulator (EI) state. A review by Pertsova and Balatsky[26] is cautiously optimistic, pointing out that in Dirac or Weyl materials the EI's transition temperature T_c could reach tens of Kelvin, and that the inversion's lifetime τ could be long. Indeed, τ is critical: time is needed for excited carriers to cool below T_c, and in order to observe the state spectroscopically the product of τ and the excitonic gap should exceed $\hbar/2$.

The hope for a long τ lies in a theoretical prediction that Auger recombination, which in graphene is fast enough to be the dominant recombination channel,[54,55] should be far slower in 3D Dirac and Weyl semimetals,[56] including in nodal-line materials.[57] (For Dirac and Weyl semimetals, as for graphene, linear dispersion causes the phase-space for Auger recombination to vanish. However, in graphene this vanishing is compensated by a diverging matrix element for scattering; in 3D materials it is not.) Opening a gap at the Dirac node[55] or doping E_F away from the node may profoundly influence the rate of Auger recombination (and of its inverse process, impact ionization, which can cause carrier multiplication).

Population inversions are known to occur even in graphene[55]—though the electron and hole chemical potentials remain distinct for only 130 fs—but few studies suggest an inversion in 3D Dirac and Weyl semimetals. In $MoTe_2$, the recombination lifetime, though just 1.5 ps, appears to exceed the cooling time of 0.38 ps.[48] In Cd_3As_2 Zhang *et al.*[35] measured the THz conductivity, finding that after photoexcitation ω_p^{scr} was enhanced, and remained so for about 6 ps. (It seems likely that N increased, rather than that ϵ_∞ decreased, since Refs. 41

and 47 show that excitation *in*creases ϵ_∞; and this excess population should not be caused merely by electron temperature, as the sample had a high E_F.) Cd_3As_2 itself is a poor candidate for an EI, as its predicted T_c is just 0.1 K, but an inversion with a similar lifetime in other Dirac or Weyl materials would be encouraging indeed.

2. Electronic cooling

Type-II Weyl semimetals such as T_d-WTe_2[11] resemble classic semimetals like Bi in having pockets of electrons and holes, whose recombination therefore requires a phonon. In both T_d-WTe_2[49] and Bi,[58] this phonon-assisted recombination is strongly temperature-dependent, is several times slower than in other Dirac and Weyl semimetals,[50] and is slower than the rate of electronic cooling.

When recombination processes are fast, on the other hand, the actual rate of recombination will match the rate at which electrons cool by giving energy to the lattice (Fig. 2e). It is well established that the pump heats the electrons by a few hundred Kelvin, and that they subsequently cool with few-picosecond time constants,[32,33,40,42,49] though some work has suggested much higher initial temperatures[36] or much faster cooling.[48]

When the few-picosecond decay of ΔR appears multi-exponential, it is tempting to attribute the distinct decay rates to distinct relaxation processes—but this temptation should be resisted. To see why, consider $\Delta R(T_e)$, which various authors have described *via* phenomenological curves,[34] minimalist models,[42] or detailed material-specific calculations.[36] Notice (Fig. 3e) that $\Delta R(T_e)$ is generally not linear, and seldom even monotonic. Thus even the simplest electronic cooling will generically result in a non-simple shape for $\Delta R(t)$. (The same may be true for metals,[59] though the relevant temperature scale is higher.)

Nonetheless, the electrons' cooling may indeed occur in distinct stages, particularly when the TTM fails. Electrons often couple more strongly to optical phonons than to acoustic, resulting in a "phonon bottleneck":[60] the optical phonons rapidly reach thermal equilibrium with the electrons, while the acoustic phonons remain cool; further electronic cooling then relies on the slower, anharmonic processes that transfer energy from optical to acoustic phonons. The description of this process requires at least three temperatures. Evidence for a phonon bottleneck in 3D Dirac and Weyl semimetals, however, is sparse[32,40]—partly because, as noted, a biexponential decay of ΔR needn't imply biexponential cooling. (Let's also note that biexponential fits should not be trusted when the two decay rates are very close, and that an experiment's interpretation should not hinge on subtle differences in the decay rate, particularly when those differences lie close to the noise level.[61])

C. Prospects for ultrafast thermodynamics

The picture of ultrafast dynamics I've presented is both simple and simplified, but describes many Dirac and Weyl semimetals under many experimental conditions. The usual pattern is this:[50] in less than a picosecond electrons thermalize with each other and begin to cool, and some of them occupy the Dirac cone. Cooling proceeds over the next few picoseconds; recombination accompanies cooling, but may be somewhat slower. This pattern continues to be borne out in new measurements and materials, recently NbAs,[42] $ZrTe_5$,[61] ZrSiSe,[47] and $EuCd_2As_2$.[62] Can anything still remain to be learned?

Consider that the detailed ultrafast description of graphene, a veritable *drosophila* for simplicity and ubiquity, has required years of theoretical and experimental effort. For 3D Dirac and Weyl semimetals, most of this effort lies ahead. Establishing the rates of thermalization, recombination, or cooling—as has largely been done—does not establish specific mechanisms, nor which populations of electrons and phonons take part. Important questions remain open: Can a population inversion exist for long enough, and at a low enough electronic temperature, to enable lasing or an exciton insulator? Does carrier multiplication take place? Does a phonon bottleneck slow the electrons' cooling? How are the dominant mechanisms of ultrafast cooling and recombination related to a material's basic properties—its Fermi energy and phonon spectrum, whether it is a Dirac, Weyl, or nodal-line semimetal, whether its node is gapped? Indeed, are such generalizations useful across this class of materials, or must each material be considered *ad hoc*?

The field would benefit from wider use of mid-IR pumps (also beneficial for nonlinear optical studies, Sec. III) and of more elaborate probes—particularly time-domain THz, transient-grating, broadband reflectivity, and ARPES. Material-specific calculations of optical properties (currently available only for a handful of materials[38,63,64]) are particularly valuable when the joint density of states is resolved by its band contributions,[38,47] and measurements of the optical conductivity are necessary to constrain the interpretation of pump-probe reflectivity experiments. Improvements in chemical or electrostatic doping would allow contrasting a material's ultrafast dynamics when E_F is near, or far from, the node.

Despite the practical and fundamental interest of ultrafast thermodynamics, these experiments have traditionally, if tacitly, been the sort that researchers do while they're working on something more interesting. Fortunately, Dirac and Weyl semimetals offer many interesting avenues for ultrafast research, discussed below, and ultrafast thermodynamics can help to propel research along these avenues.

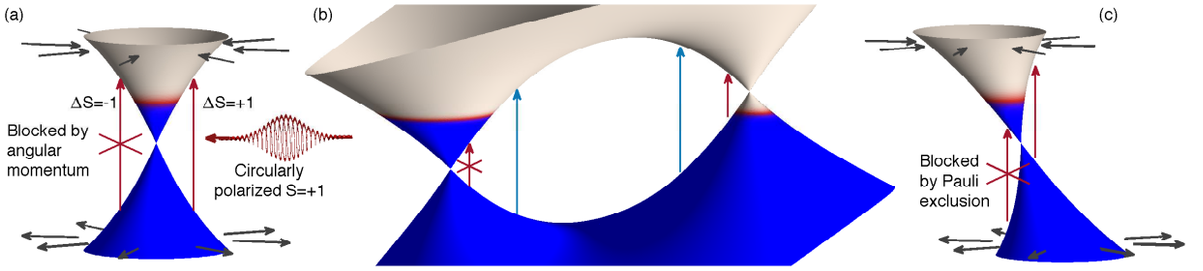

FIG. 4. **(a)** The chiral dispersion of a single Weyl node, plus conservation of angular momentum, leads to a nonzero, spin-polarized photocurrent on absorption of a circularly-polarized photon. Gray arrows indicate spin. **(b)** In a material with a chiral crystal structure, the different energies of Weyl points allow just one chirality of Weyl node to contribute to the photocurrent. (Low-energy excitation, red arrows). For higher-energy photons (blue arrows), the two opposite-chirality Weyl points may cancel each other's effects. **(c)** A tilted Weyl dispersion, as in TaAs, gives nonzero photocurrent. To understand why the photocurrent from multiple tilted Weyl nodes does not cancel, see the supplement to Ref. 65. Figures inspired by Refs. 65–67.

III. PHOTOCURRENTS IN WEYL SEMIMETALS

A material's second-order response to a short optical pulse can include the brief flow of a dc photocurrent proportional to the incident intensity, known as the photogalvanic effect (PGE). The current[68] is commonly measured by detecting emission of terahertz radiation from the sample, through difference-frequency generation between frequencies present in the optical pulse. The complimentary, sum-frequency process results in the flow of photocurrent, and the emission of light, at double the incident frequency. Darius Torchinsky describes this process of second-harmonic generation (SHG) as "two photons enter, one photon leaves."[69] Both PGE and SHG must vanish in centrosymmetric materials, such as Dirac semimetals, except at the surface.

Weyl semimetals are too absorptive in the visible range to replace standard crystals like ZnTe for SHG applications, but applications of their PGE are promising: the photocurrent flows even without an applied bias, which could reduce dark-current noise in mid-IR optical detectors.[23] The photocurrent's dependence on the incident polarization allows facile control of the circular and elliptical polarization of the emitted THz,[70] and its sensitivity to phase gradients allows detection of the orbital angular momentum of light.[71]

The study of SHG and PGE in Weyl semimetals has proved both alluring and treacherous. The allure stems from the prospect of relating the photocurrent to the electronic topology. While the linear electromagnetic responses of Weyl semimetals—those proportional to $\vec{E}$, such as the conductivity—don't have unique features of topological origin, the nonlinear responses may.[67] (For instance the chiral anomaly, the classic signature of Weyl physics, is second-order, being proportional to $\vec{E} \cdot \vec{B}$.) Each Weyl point acts as a monopole of Berry curvature, and under circularly-polarized illumination (Fig. 4a) leads to photocurrent injection at a rate, β, quantized by the fundamental constants e and $\hbar$.[72]

Photocurrents in Weyl semimetals arise from interband optical transitions, and fall into two classes, which cause circular and linear PGEs.[73,74] The *injection current* occurs upon absorption of circularly polarized light. Because of differences in the band dispersions of the initial and final states, each photoexcited electron receives a "kick" that changes its velocity. The *shift current* occurs upon absorption of linearly polarized light. An electron's initial and final states may have different center-of-mass positions within the unit cell, and the abrupt change in position constitutes a current. Topology influences both types of photocurrent, with the injection current related to the bands' Berry curvature and the shift current related to the Berry connection between bands.

The treacheries, however, are legion. First, electron-electron interactions may destroy the photocurrent's quantization.[75] Second, neither the linear nor the circular PGE must necessarily have a topological origin: the shift current may be zero even when the Berry connection is nonzero,[74] and the linear PGE needn't arise solely from shift current, but may also come from asymmetric scattering off of defects or phonons;[76] similarly, circular PGE occurs in many non-topological materials (see citations in Ref. 66). Third, a condition necessary for PGEs and SHG—that the crystal lack inversion symmetry—is also necessary for all non-magnetic Weyl semimetals, making it difficult to distinguish the effects of topology from those of symmetry. Finally, Weyl points come in pairs of opposite chirality, whose contributions to β cancel, eliminating the quantized current injection. Overcoming this cancellation requires a chiral crystal (one lacking any mirror planes); only then may the Weyl points lie at different energies. These energies will define a frequency range of quantized photocurrent, in which only Weyl points of one chirality contribute (Fig. 4b).

Chiral Weyl semimetals are elusive,[77] so the quantized PGE has been sought in the related "multifold" semimetals RhSi[12,64,66] and CoSi[77]—sought, but not found. The injection current decays with hot-electron momentum-

relaxation time τ_p, and too short of a τ_p will prevent quantization of β, as may some values of the Fermi energy or transitions between non-topological bands. Deficiencies in these material properties have conspired to hide the quantized photocurrent in all experiments to date. (The topological, albeit non-quantized, nature of the photocurrent does manifest itself in RhSi,[66] where a plateau in $\beta\tau_p$ below 0.65 eV and its suppression above that energy seems to herald the crossover of the effective Berry charge from nonzero to zero—see Fig. 4b.)

The relation of PGEs to topology is similarly fraught in TaAs, an intensively-studied, non-chiral Weyl semimetal.[65,70,73,76,78–80] Pairs of opposite-chirality Weyl points sit at equal energies, and their contributions to the PGE ought to cancel,[67] but tilt or curvature of the Weyl cones makes the cancellation imperfect (Fig. 4c). Injection current observed under mid-IR illumination arises from interband excitations within these tilted Weyl cones,[65] but may not be topological in origin, as the photocurrent behaves similarly for 1.55-eV excitation, well beyond the topologically-relevant range of the Weyl bands.[79] The SHG is remarkably large,[76,78] being resonantly enhanced by a strong interband transition—but is unrelated to topology, deriving instead from shift currents due to the crystal's polar character.[73,76]

A. Ultrafast progress and prospects

Most SHG and THz-emission experiments described above used ultrafast optical pulses but did not time-resolve the response. THz emission in principle can measure the time-dependence of excited photocurrents, but only if the bandwidths of the excitation pulse and THz-detection system both exceed the photocurrent decay rate $1/\tau_p$,[79] which they rarely do. High-bandwidth measurement could help in observing the quantization of β: the injection current measured by THz emission is proportional to $\beta\tau_p$, so the hot-electron lifetime τ_p must be known accurately to infer β. (In Ref. 66, uncertainty in τ_p contributed to an order-of-magnitude uncertainty in β.) Conventional pump-probe studies would help, too—they could be used to measure the energy-dependent τ_p under experimentally relevant conditions. Ultrafast methods may also help to quantify the role of interactions in degrading the quantization of the photocurrent.[75]

Time-resolved SHG also offers several advances. A strong THz pump pulse may produce symmetry-breaking currents, which are predicted to allow large SHG even in centrosymmetric materials like Dirac or magnetic Weyl semimetals.[81] Sirica *et al.*[80] showed that an 800-nm pump pulse, when incident on certain faces of TaAs, can induce a photocurrent that breaks crystalline symmetries, as inferred from sub-picosecond changes to the detected SHG. This current is expected to modify the locations of the Weyl points and the surface Fermi arcs, and thus may offer ultrafast control of topological properties. Other time-resolved SHG experiments[82,83] have revealed pump-induced lattice deformations that can restore inversion symmetry to T_d-WTe_2 and $MoTe_2$—another possible route to ultrafast control of topology, discussed in the next section.

IV. ULTRAFAST CONTROL

Perhaps the most exciting application of ultrafast optics to topological materials is not to measure their properties, but to rapidly control their band topology, for instance by splitting a Dirac node into a pair of Weyl nodes, or by opening a gap at the Dirac point. Such ultrafast control could enable experiments investigating new physics or, more speculatively, might rapidly switch a "topological field effect transistor."[84] Reversible control of the band topology or the nodal gap may provide an ultrafast on-off switch for the exotic optical effects described in Section I, or allow researchers to create Dirac fermions on demand and to create and tune electronic states beyond those available in static materials. Two principal methods, with complementary strengths and weaknesses, are being pursued to allow ultrafast optical pulses to control topological materials. The pulses can act on the band structure directly through their electric field, or indirectly through coherent phonons or photoexcited electrons.

A. Floquet effects

The most prominent theoretical proposals for ultrafast control of Dirac and Weyl materials employ Floquet effects. (See, e.g., the lovely review by De Giovannini and Hübener.[87]) Floquet theory obtains a material's behavior under a time-periodic external field, and has recently proven very successful, showing that an optical pump may radically change the band structure and topological nature of materials.

When a pump pulse is incident on a material, its electric field periodically modulates the Hamiltonian: $\hat{H} = \hat{H}_0 + \hat{P}e^{i\omega t} + \hat{P}^\dagger e^{-i\omega t}$, where $\hat{H}_0$ is the material's original Hamiltonian, and ω is the pump frequency. Just as a crystal's spatially periodic potential makes its electronic dispersion $E(\vec{k})$ periodic in the quasi-momentum $\vec{k}$, time periodicity leads to a spectrum periodic in the quasi-energy, forming a ladder of "replica" bands: $E_n(\vec{k}) = E(\vec{k}) + n\hbar\omega$. Though in general none of these bands equals those of $\hat{H}_0$, we can define the zero-harmonic ($n = 0$) Floquet-Bloch bands $E(\vec{k})$ as those that most closely follow the original bands—and which typically have the greatest spectral weight (Fig. 5a,b). In the limit of large ω, the $n = 0$ bands and their corresponding eigenstates are given by the simple effective Hamiltonian $\hat{H}_{\text{eff}} = \hat{H}_0 + \frac{1}{\omega}[\hat{P}^\dagger, \hat{P}]$, which affords an analytic expression for $\hat{H}_{\text{eff}}$ and allows the photon-dressed material to be classified in terms of topology.

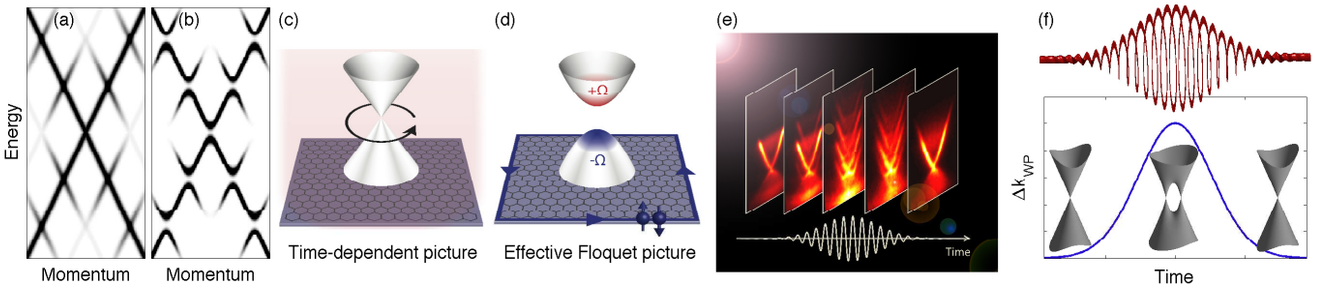

FIG. 5. **(a), (b)** Representation of a Dirac cone along with its Floquet-Bloch replica bands, without (a) or with (b) gaps opened at the band crossings. **(c), (d)** The interaction between graphene and circularly polarized light, as seen with a time-dependent Hamiltonian (c) or in the Floquet picture (d), which includes a topological band gap with Berry curvature Ω. **(e)** Time-resolved ARPES images of Floquet-Bloch surface states of Bi_2Se_3, and their interaction with free-electron Volkov states.[85] (courtesy Fahad Mahmood). **(f)** A circularly-polarized pulse is predicted to split a 3D Dirac cone into two Weyl cones whose $\vec{k}$-space separation Δk_{WP} depends on the light's intensity, leading to the "dancing" Weyl points described in Ref. 9. Panels (c) and (d) reprinted by permission from *Nature Physics* **16** 38 (2020)[86].

The effects on topology may be profound. By shifting the dispersion, the pump may create new inversions, crossings, or avoided crossings between zero-harmonic bands or replica bands; some of these crossings may form Dirac or Weyl points. Critically, the new bands and their crossing points may acquire a Berry curvature not present in the original bands.[88,89] Circular polarization is particularly important, as explained by Oka and Aoki:[88] the optical field causes each $\vec{k}$-space point to follow a circle in the Brillouin zone, and those points that circumnavigate a Dirac point acquire an additional, nontrivial phase (Fig. 5c,d). Alternately, one can think of circularly polarized light as breaking time-reversal symmetry—a particularly apt picture when, like a magnetic field, it has the effect of gapping the surface states of a topological insulator[90] or of splitting a Dirac point into two Weyl points.[8,9,27,28]

The amplitude A of the optical field is an important tuning parameter, and Floquet-Dirac and Floquet-Weyl materials are predicted to have rich phase diagrams in the $A-\omega$ plane. For instance, at low amplitude an optical field may split a Dirac point into two Weyl points; as the amplitude increases, The Weyl points may move so far in $\vec{k}$-space that they pair-annihilate and are gapped.[8]

Such theoretical work has been encouraged by two seminal experiments on 2D systems. Wang *et al.*[90] studied the surface states of the topological insulator Bi_2Se_3, demonstrating that during illumination by a strong infrared pulse, new nodes appear at the crossings of Floquet-Bloch replica bands (Fig. 5e).[85] The nodes could be gapped or gapless, for circularly- or linearly-polarized light, respectively. A recent experiment on graphene extended the evidence for Floquet effects from spectroscopic signatures to transport. McIver *et al.*[86] used Auston switches coupled to transmission lines to measure the time dependence of the anomalous Hall effect—the Hall current in the absence of a magnetic field. They found it to be zero except during a circularly-polarized pump pulse (and perhaps for a few picoseconds after), when it was nonzero and possibly quantized. The work confirmed a classic prediction of Floquet theory:[88] that a circular pump opens a gap at the Dirac point, with Berry curvature induced at the band edges (Fig. 5c,d). There have also been experimental successes on 2D material analogues—cold-atom[91] and photonic[92] systems.

A large body of theory now extends Floquet ideas to 3D Dirac and Weyl semimetals. Ultrafast pulses are predicted to convert a topologically trivial insulator to a 3D Dirac semimetal[93] and *vice versa*, and to open[9] or close[29] a gap at the node of a Dirac semimetal. Other proposals, rather than controlling a gap, would control the spin-degeneracy of a node: circularly-polarized light is predicted to introduce Weyl points into the bulk of topological insulators,[94] Dirac semimetals[8,9,27,28] (Fig. 5f), or nodal-line materials.[28,30] The overall impression is of a boundless alchemy.

No experiment, however, has yet confirmed these predictions. Sample damage has likely been a major impediment to progress on 3D materials, since Floquet effects require a strong peak electric field. (Ref. 90 succeeded, in part, because the bulk states of topological insulators, unlike those of 3D semimetals, are gapped. The sub-gap infrared pump pulse could be absorbed only at the surface, limiting sample damage.) Another challenge is that the few experiments currently known to give clear signatures of Floquet effects, ultrafast ARPES[85,90] and utrafast transport, both with mid-IR pump pulses, are extraordinarily difficult.

The few successes in 2D have nourished the theory community, but are thin soup for solid-state experimentalists. Though the basic results of Floquet theory are not in doubt, experiments remain important, because theory has only rarely treated a realistic Hamiltonian for a specific material.[9] Additionally, as Kitagawa *et al.*[95] point out, some topological properties appear only when certain bands are fully filled. Considering that after photoexcitation electrons and holes promptly find their way to the vicinity of the node,[39–41] it cannot be supposed *a*

priori that even non-resonant excitation will leave topological properties intact. Finally, verifying predictions is only a beginning; achieving ultrafast control of Dirac and Weyl materials would open whole new frontiers to exploration.

B. Coherent phonons

Since electronic band structure depends sensitively on atoms' positions within a crystal, phonons provide an alternate method for ultrafast control of topological materials. A short optical pulse can launch a coherent phonon, in which the atoms' positions oscillate in sync with each other. Within the "frozen-phonon" approximation—in which the electronic dispersion instantaneously adjusts to a new lattice configuration[96,97]—the result can be band topology that oscillates at the phonon's frequency, much like the "flickering" surface-state Dirac cones predicted in topological crystalline insulators.[98]

Coherent phonons complement Floquet effects in several ways. The atoms' oscillation may be started by one laser pulse, and then either amplified or stopped by a subsequent pulse, and may continue to periodically modulate the bands even after the excited carriers have recombined. Coherent phonons are band-selective, with different bands sensitive to different phonon modes.[99] The intra-unit-cell strains exerted by coherent phonons without damaging a crystal may greatly exceed typical uniaxial strains.[82,100] Techniques of "nonlinear phononics" (Section IV C) may excite coherent phonons accompanied by minimal electronic excitation, or may rectify a phonon's motion.[100,101]

Several 3D topological semimetals, notably $SrMnSb_2$, T_d-WTe_2, $MoTe_2$, and $ZrTe_5$, are now strong candidates for coherent-phonon-based control. For each material, at least one phonon mode is predicted to modify the band topology, either by breaking (or restoring) a symmetry, or by modifying the bands' inversions.

$SrMnSb_2$ (Fig. 6a) is a Dirac semimetal that, were it tetragonal, would have a gapless Dirac dispersion at the Y-point. Instead, it suffers a Peierls-like distortion that renders it orthorhombic and that gaps the Dirac node by about 200 meV. Like the Peierls-distorted semimetals Bi and Sb,[102] $SrMnSb_2$ is highly susceptible to the excitation of coherent phonons that act to partially repair the structural distortion, and 800-nm pulses readily excite a 4.4-THz, A_g mode.[103] Calculations show that as this phonon's displacement increases, the nodal gap narrows and eventually closes. For sufficiently high oscillation amplitudes it should be possible to periodically close and open the gap once per phonon oscillation, as illustrated schematically in Fig. 6a.

WTe_2, in its T_d phase, (Fig. 6b) is a type-II Weyl semimetal with a non-centrosymmetric structure.[11] Ultrafast pulses can excite the coherent oscillation of a 0.24-THz, interlayer shear-mode phonon.[49,104] Displacement of this mode by $\Delta x = 12$ pm would place the crystal into the metastable, centrosymmetric $1T'(^*)$ structure,[105] where Weyl points cannot exist. Sie and Nyby *et al.*[82] used a terahertz pump and ultrafast electron-diffraction (UED) probe to demonstrate coherent oscillations of this mode with amplitudes of $\Delta x > 4$ pm, and showed theoretically that two opposite-chirality Weyl points should merge when $\Delta x = 2.2$ pm, even before reaching $1T'(^*)$. When driven still more strongly, the crystal appeared to gradually reach the centrosymmetric phase, where it remained for nanoseconds. Similar behavior is expected, and may have been observed, in $MoTe_2$.[83]

Hein *et al.*[99] observed the effect of this phonon's motion on the electronic dispersion though ultrafast ARPES, with displacements of $\Delta x \approx 1$ pm. Though the Weyl points have too small of energy- and momentum-scales to be observed directly in ARPES, outside the Weyl region the band energies were seen to oscillate, as was the spin-splitting of the bands that form the opposite-chirality Weyl points—as theoretically expected[106] when the Weyl points merge.

$ZrTe_5$ (Fig. 6c,d) is typically a strong topological insulator (STI), but small changes in the lattice parameters can render it a weak topological insulator (WTI). At the STI-to-WTI transition, $ZrTe_5$ becomes a "fine-tuned" 3D Dirac semimetal, with a Dirac cone at the Γ point. Even slight changes in sample growth conditions, temperature, or strain can induce transitions among these three phases.[107,108] Thus poised, $ZrTe_5$ is an exquisite candidate (if a temperamental one) for topological control by several different coherent phonons. Calculations[109] have identified five A_g phonon modes that, at sufficient amplitude, may oscillate the material from STI to WTI and back, briefly forming a Dirac semimetal at a critical atomic displacement; linear combinations of these modes may also induce the transition. These A_g modes preserve the crystal's inversion symmetry, but modify the inversion of the valence and conduction bands.[109]

Experiments using a terahertz pump[110] have excited the coherent oscillation of one such phonon. In other experiments, UED showed slow atomic motion (tens of picoseonds) along the directions of these same phonons.[111] (The motion did not appear to oscillate coherently, perhaps due to the time-resolution of UED.) Other calculations[112] identified an inversion-breaking, B_{1u} phonon that would turn $ZrTe_5$ into a Weyl semimetal, splitting the Dirac point into two pairs of Weyl points. The momentum-space separation $\Delta\vec{k}$ of these points would oscillate along with the phonon's displacement; more interesting still, changes in $\Delta\vec{k}$ would change the connectivity of the surface Fermi arcs, which would flicker back and forth across momentum space.

C. The path to ultrafast control

Beyond coherent-phonon and Floquet effects, two other routes to ultrafast control of topological properties deserve mention. Photocurrent-driven transient symme-

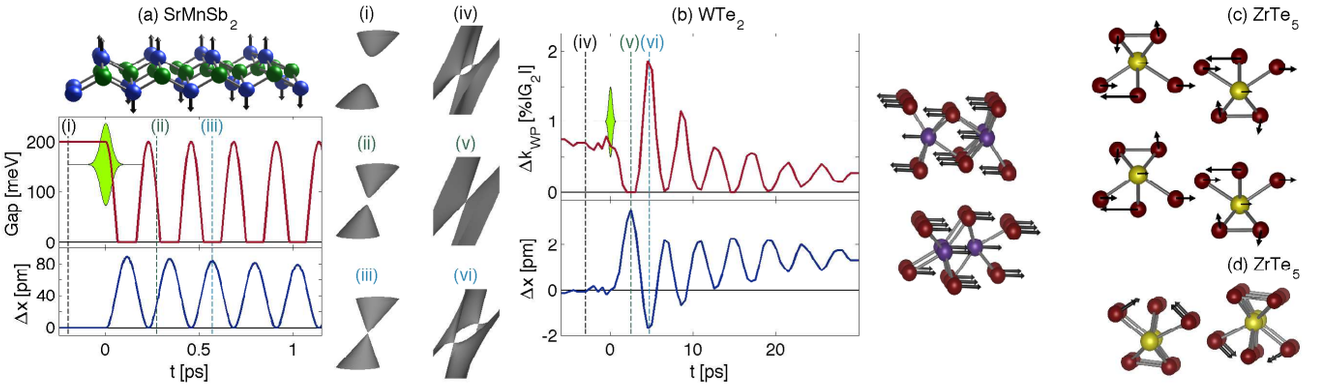

FIG. 6. **(a)** Illustration of Sb and Mn planes during oscillation of the 4.4-THz breathing mode of $SrMnSb_2$. Schematic portrayal of how of a high-amplitude oscillation, $\Delta x(t)$, might close the gap in the Dirac cone after an optical pump (chartreuse). (i)-(iii) and (iv)-(vi) illustrate the Dirac and Weyl nodes corresponding to the times labeled on plots (a) and (b). **(b)** Illustration of the shear-mode phonon and its influence on Weyl nodes in T_d-WTe_2. The atomic displacement $\Delta x(t)$ caused by a 23-THz pump pulse (chartreuse) is measured by UED, and the corresponding $\vec{k}$-space separation of Weyl points Δk_{WP} is calculated from Δx. The units of Δk_{WP} are percent of the reciprocal-lattice vector $\vec{G}_2$ (Data from Ref. 82, courtesy of Aaron Lindenberg.) **(c)** The B_{1u} phonon predicted to turn $ZrTe_5$ into a Weyl semimetal (courtesy of Linlin Wang). **(d)** A semaphore-mode A_g phonon, one of several predicted to tune $ZrTe_5$ between Dirac semimetal and topological insulator (courtesy of Weiguo Yin). (Color code: Sb blue; Mn green; Te burgundy; W aubergine; Zr mustard.)

try breaking[80,81] (Sec. III A) warrants further theoretical elaboration: what specific changes to the Dirac or Weyl points and the surface Fermi arcs are achievable in TaAs, Cd_3As_2, $Co_3Sn_2S_2$, and other materials? Another proposal regards the pyrochlore iridates, which are antiferromagnetic insulators. After an optical pulse, screening by photoexcited electrons would reduce the magnetization to the point that the material would become a Weyl semimetal, which would persist as long as the excited population remained sufficiently high.[113]

Implementing any of these methods of ultrafast control presents significant experimental challenges. None is yet supported by direct spectroscopic evidence in 3D semimetals, so ultrafast ARPES will be crucial—but for some materials the relevant energy scales are prohibitively small.[99] For photocurrent-driven transient symmetry breaking, THz pumping will often be needed.[81] If coherent phonons are used, the atomic displacements must be measured quantitatively, which to date has been done only for T_d-WTe_2 among these materials.[82] Ultrafast diffraction will usually be necessary, though broadband reflectivity may sometimes suffice if supported by reliable calculations.[114]

The excitation processes, too, must be characterized and explored. Except in Ref. 113, the electrons, holes, and incoherent phonons that accompany photoexcitation are undesirable—necessitating study of the rates and mechanisms of their decay (Sec. II), and methods for exciting a sample while minimally exciting carriers. For coherent phonons, the amplitudes required may be large (52 pm in $SrMnSb_2$), and though displacements of this order are not unprecedented[115] high laser fluences will be necessary. Some aid may come from the flourishing field of nonlinear phononics,[101,116] which exploits the couplings between phonons. Resonant absorption can strongly drive infrared-active modes, which may be coupled to Raman-active modes by sum- and difference-frequency processes, resulting for instance in rectification (unidirectional displacement) of the Raman-active mode. This field has seen dramatic success in the manipulation of superconductors,[117,118] ferroelectrics,[119] and magnets,[100,120] but has not, to my knowledge, been applied to topological materials.

The importance of strong laser pulses for both coherent-phonon and Floquet-based proposals puts a premium on knowing the materials' damage thresholds. An experiment that gingerly approaches the damage threshold from below wastes beamtime; one that rashly approaches it from above wastes samples. Researchers should include information about damage thresholds, where available, in their publications,[121] and for important materials systematic studies of damage should be undertaken. Similarly, negative results should be considered publishable. Considering the many dramatic predictions of Floquet effects in 3D materials, and the paucity of their experimental support, it is a near certainty that many failed experimental attempts lie unpublished—and, sadly, that other researchers are repeating the same failures.

V. FINAL CONSIDERATIONS

The preceding sections have indicated opportunities and challenges facing ultrafast research on Dirac and Weyl semimetals. I have discussed some of the experimental and theoretical work needed to advance the field. Two final experimental needs deserve mention.

The great engine driving research on Dirac and Weyl semimetals has been materials synthesis. Ultrafast research will benefit both from the discovery of new materials and from improvements in their quality. For instance, observing quantized injection of photocurrent will require control of E_F and reduction of impurity scattering, and possibly even the discovery of new Weyl or multifold semimetals with chiral crystal structures.

Wider availability of thin films would be particularly useful. Beyond their general advantages—the tuning of epitaxial strain, incorporation into multilayer structures, and surface doping—films' large, flat surfaces facilitate grazing-incidence measurement, useful for instance in ultrafast X-ray diffraction. In experiments where the probe's absorption length exceeds the pump's (e.g. an optical pump with an X-ray probe) the film's thickness can be matched to the pump's absorption length—typically tens of nanometers—to allow measurement of a nearly uniformly-excited sample. A thickness comparable to the probe's absorption length is ideal for measurements of transmission, and could enable observation of resonant transparency,[19] tunable passbands,[20] and other exotic optical phenomena. Films allow measurement of the THz conductivity, which may probe energies within the Dirac and Weyl cones.

Finally, the magnetic Weyl semimetals,[13,14] in which the existence of Weyl points depends on breaking time-reversal symmetry, remain largely unexplored by ultrafast techniques.[122,123] A rich field of study is practically assured: magneto-optical probes readily lend themselves to imaging and to ultrafast time-resolution, and will be particularly useful in the mid-infrared.[124] Optical pump pulses are known to induce magnetic precession[122] or demagnetization,[123] suggesting the possibility of ultrafast magnetic control of Weyl physics. Moreover, magnetic materials frequently sport complex phase diagrams, strong electronic correlations, hysteresis, exchange bias at interfaces, and textures[13] such as domain walls and skyrmions that needn't be static. An experimenter entering so broad and untracked a parameter-space may wish to leave a trail of bread-crumbs behind.

Though the ultrafast dynamics of Dirac and Weyl semimetals might seem to be of purely parochial interest, its consequences are cosmopolitan. The rates and mechanisms of electronic relaxation are relevant not only to device operation but also to the prospects for studying the exciton insulator or Floquet effects—both topics of sufficient fundamental interest to have sustained vigorous theoretical work despite limited experimental success. Quantized injection of photocurrent, if observed, would join the highly exclusive company of experimental phenomena distinctive to Weyl semimetals. Achieving ultrafast, on-off control of Dirac or Weyl points, whether by coherent phonons or by Floquet effects, would enable the investigation of optical properties and electronic states without parallel in static experiments. Ultrafast dynamics of Dirac and Weyl semimetals is just embarking on a great journey of discovery.

VI. ACKNOWLEDGEMENTS

I am grateful for helpful discussions with Alexander Afanasiev, Michael Bauer, Dominik Juraschek, Erin Knutson, Takashi Oka, Nicholas Sirica, and Darius Torchinsky. I acknowledge NSF-DMR-1904726.

VII. DATA AVAILABILITY

Data sharing is not applicable to this article as no new data were created or analyzed in this study.

[1] T. Liang, Q. Gibson, M. N. Ali, M. Liu, R. J. Cava, N. P. Ong, Ultrahigh mobility and giant magnetoresistance in the Dirac semimetal Cd_3As_2. *Nat. Mater.* **14**, 280-284 (2015).
[2] A. A. Burkov, Topological semimetals. *Nature Materials* **15**, 1145–1148 (2016).
[3] E. Derunova, Y. Sun, C. Felser, S. S. P. Parkin, B. Yan, M. N. Ali, Giant intrinsic spin Hall effect in W_3Ta and other A15 superconductors. *Science Advances* **5** (2019).
[4] D. E. Kharzeev, H.-U. Yee, Anomaly induced chiral magnetic current in a Weyl semimetal: Chiral electronics. *Phys. Rev. B* **88**, 115119 (2013).
[5] K. Inzani, A. Faghaninia, S. M. Griffin, Prediction of tunable spin-orbit gapped materials for dark matter detection. *arXiv:2008.05062v1* (2020).
[6] B. Yan, C. Felser, Topological materials: Weyl semimetals. *Annual Review of Condensed Matter Physics* **8**, 337-354 (2017).
[7] N. P. Armitage, E. J. Mele, A. Vishwanath, Weyl and Dirac semimetals in three-dimensional solids. *Rev. Mod. Phys.* **90**, 015001 (2018).
[8] L. Bucciantini, S. Roy, S. Kitamura, T. Oka, Emergent Weyl nodes and Fermi arcs in a Floquet Weyl semimetal. *Phys. Rev. B* **96**, 041126 (2017).
[9] H. Hübener, M. A. Sentef, U. De Giovannini, A. F. Kemper, A. Rubio, Creating stable Floquet–Weyl semimetals by laser-driving of 3D Dirac materials. *Nat. Commun.* **8** (2017).
[10] L. M. Schoop, M. N. Ali, C. Straßer, T. Andreas, V. Andrei, D. Marchenko, V. Duppel, S. S. Parkin, B. V. Lotsch, C. R. Ast, Dirac cone protected by non-symmorphic symmetry and three-dimensional Dirac line node in ZrSiS. *Nat. Commun.* **7**, 11696 (2016).
[11] A. A. Soluyanov, D. Gresch, Z. Wang, Q. Wu, M. Troyer, X. Dai, B. A. Bernevig, Type-II Weyl semimetals. *Nature* **527**, 495–498 (2015).
[12] G. Chang, S.-Y. Xu, B. J. Wieder, D. S. Sanchez, S.-M. Huang, I. Belopolski, T.-R. Chang, S. Zhang, A. Bansil, H. Lin, M. Z. Hasan, Unconventional chiral fermions and large topological Fermi arcs in RhSi. *Phys. Rev. Lett.* **119**, 206401 (2017).
[13] Y. Araki, Magnetic textures and dynamics in magnetic Weyl semimetals. *Annalen der Physik* **532**, 1900287 (2020).
[14] W. Ning, Z. Mao, Recent advancements in the study of intrinsic magnetic topological insulators and magnetic Weyl semimetals. *APL Materials* **8**, 090701 (2020).
[15] B.-J. Yang, N. Nagaosa, Classification of stable three-dimensional Dirac semimetals with nontrivial topology. *Nature Communications* **5**, 4898 (2014).
[16] A. V. Pronin, M. Dressel, Nodal semimetals: A survey on optical conductivity. *physica status solidi (b)* p. 2000027 (2020).
[17] P. E. C. Ashby, J. P. Carbotte, Chiral anomaly and optical absorption in Weyl semimetals. *Phys. Rev. B* **89**, 245121 (2014).
[18] J. M. Shao, G. W. Yang, Photoconductivity in Dirac materials. *AIP Adv.* **5**, 117213 (2015).
[19] Y. Baum, E. Berg, S. Parameswaran, A. Stern, Current at a distance and resonant transparency in Weyl semimetals. *Phys. Rev. X* **5**, 041046 (2015).

[20]O. V. Kotov, Y. E. Lozovik, Dielectric response and novel electromagnetic modes in three-dimensional Dirac semimetal films. *Phys. Rev. B* **93**, 235417 (2016).
[21]C. Zhu, F. Wang, Y. Meng, X. Yuan, F. Xiu, H. Luo, Y. Wang, J. Li, X. Lv, L. He, Y. Xu, Y. Shi, R. Zhang, S. Zhu, A robust and tuneable mid-infrared optical switch enabled by bulk Dirac fermions. *Nat. Commun.* **8**, 14111 (2017).
[22]M. Yang, J. Wang, Y. Yang, Q. Zhang, C. Ji, G. Wu, Y. Su, J. Gou, Z. Wu, K. Yuan, F. Xiu, Y. Jiang, Ultraviolet to long-wave infrared photodetectors based on a three-dimensional Dirac semimetal/organic thin film heterojunction. *J. Phys. Chem. Lett.* **10**, 3914-3921 (2019).
[23]J. Liu, F. Xia, D. Xiao, F. J. García de Abajo, D. Sun, Semimetals for high-performance photodetection. *Nature Materials* **19**, 830–837 (2020).
[24]B. Cheng, N. Kanda, T. N. Ikeda, T. Matsuda, P. Xia, T. Schumann, S. Stemmer, J. Itatani, N. P. Armitage, R. Matsunaga, Efficient terahertz harmonic generation with coherent acceleration of electrons in the Dirac semimetal Cd_3As_2. *Phys. Rev. Lett.* **124**, 117402 (2020).
[25]S. Almutairi, Q. Chen, M. Tokman, A. Belyanin, Four-wave mixing in Weyl semimetals. *Phys. Rev. B* **101**, 235156 (2020).
[26]A. Pertsova, A. V. Balatsky, Dynamically induced excitonic instability in pumped Dirac materials. *Annalen der Physik* **532**, 1900549 (2020).
[27]S. Ebihara, K. Fukushima, T. Oka, Chiral pumping effect induced by rotating electric fields. *Phys. Rev. B* **93**, 155017 (2016).
[28]C.-K. Chan, Y.-T. Oh, J. H. Han, P. A. Lee, Type-II Weyl cone transitions in driven semimetals. *Phys. Rev. B* **94**, 121106 (2016).
[29]O. V. Kibis, K. Dini, I. V. Iorsh, I. A. Shelykh, All-optical band engineering of gapped Dirac materials. *Phys. Rev. B* **95**, 125401 (2017).
[30]Z. Yan, Z. Wang, Tunable Weyl points in periodically driven nodal line semimetals. *Phys. Rev. Lett.* **117**, 087402 (2016).
[31]S. S. Kubakaddi, T. Biswas, Hot electron cooling in Dirac semimetal Cd_3As_2 due to polar optical phonons. *Journal of Physics: Condensed Matter* **30**, 265303 (2018).
[32]C. P. Weber, E. Arushanov, B. S. Berggren, T. Hosseini, N. Kouklin, A. Nateprov, Transient reflectance of photoexcited Cd_3As_2. *Appl. Phys. Lett.* **106**, 231904 (2015).
[33]C. Zhu, X. Yuan, F. Xiu, C. Zhang, Y. Xu, R. Zhang, Y. Shi, F. Wang, Broadband hot-carrier dynamics in three-dimensional Dirac semimetal Cd_3As_2. *Applied Physics Letters* **111**, 091101 (2017).
[34]W. Lu, S. Ge, X. Liu, H. Lu, C. Li, J. Lai, C. Zhao, Z. Liao, S. Jia, D. Sun, Ultrafast relaxation dynamics of photoexcited Dirac fermion in the three dimensional Dirac semimetal cadmium arsenide. *Phys. Rev. B* **95**, 024303 (2017).
[35]W. Zhang, Y. Yang, P. Suo, W. Zhao, J. Guo, Q. Lu, X. Lin, Z. Jin, L. Wang, G. Chen, F. Xiu, W. Liu, C. Zhang, G. Ma, Ultrafast photocarrier dynamics in a 3D Dirac semimetal Cd_3As_2 film studied with terahertz spectroscopy. *Applied Physics Letters* **114**, 221102 (2019).
[36]G. Zhai, C. Ma, J. Xiang, J. Ye, T. Li, Y. Li, P. Sun, G. Chen, X. Wu, X. Zhang, Mid-infrared transient reflectance study of the Dirac semimetal Cd_3As_2 under strong optical pumping. *Phys. Rev. B* **101**, 174310 (2020).
[37]M. Marsi, Ultrafast electron dynamics in topological materials. *physica status solidi (RRL) – Rapid Research Letters* **12**, 1800228 (2018).
[38]J. Ebad-Allah, J. F. Afonso, M. Krottenmüller, J. Hu, Y. L. Zhu, Z. Q. Mao, J. Kuneš, C. A. Kuntscher, Chemical pressure effect on the optical conductivity of the nodal-line semimetals ZrSiY (Y =S, Se, Te) and ZrGeY (Y = S, Te). *Phys. Rev. B* **99**, 125154 (2019).
[39]G. Manzoni, A. Sterzi, A. Crepaldi, M. Diego, F. Cilento, M. Zacchigna, P. Bugnon, H. Berger, A. Magrez, M. Grioni, F. Parmigiani, Ultrafast optical control of the electronic properties of $ZrTe_5$. *Phys. Rev. Lett.* **115**, 207402 (2015).
[40]Y. Ishida, H. Masuda, H. Sakai, S. Ishiwata, S. Shin, Revealing the ultrafast light-to-matter energy conversion before heat diffusion in a layered Dirac semimetal. *Phys. Rev. B* **93**, 100302(R) (2016).
[41]G. Gatti, *et al.*, Light-induced renormalization of the Dirac quasiparticles in the nodal-line semimetal ZrSiSe. *Phys. Rev. Lett.* **125**, 076401 (2020).
[42]C. P. Weber, L. M. Schoop, S. S. P. Parkin, R. C. Newby, A. Nateprov, B. Lotsch, M. B. M. Krishna, J. M. Kim, K. M. Dani, H. A. Bechtel, E. Arushanov, M. Ali, Directly photoexcited Dirac and Weyl fermions in ZrSiS and NbAs. *Applied Physics Letters* (2018).
[43]M. M. Jadidi, M. Kargarian, M. Mittendorff, Y. Aytac, B. Shen, J. C. Knig-Otto, S. Winnerl, N. Ni, A. L. Gaeta, T. E. Murphy, H. D. Drew, Optical control of chiral charge pumping in a topological Weyl semimetal. *arXiv:1905.02236* (2019).
[44]B. R. Bennett, R. A. Soref, J. A. Del Alamo, Carrier-induced change in refractive index of InP, GaAs and InGaAsP. *IEEE Journal of Quantum Electronics* **26**, 113-122 (1990).
[45]A. V. Kuznetsov, C. J. Stanton, Coherent phonon oscillations in GaAs. *Phys. Rev. B* **51**, 7555–7565 (1995).
[46]A. Othonos, Probing ultrafast carrier and phonon dynamics in semiconductors. *Journal of Applied Physics* **83**, 1789-1830 (1998).
[47]R. J. Kirby, A. Ferrenti, C. Weinberg, S. Klemenz, M. Oudah, S. Lei, C. P. Weber, D. Fausti, G. D. Scholes, L. M. Schoop, Transient Drude response dominates near-infrared pump-probe reflectivity in nodal-line semimetals ZrSiS and ZrSiSe. *The Journal of Physical Chemistry Letters* **11**, 6105-6111 (2020).
[48]A. R. Attar, H.-T. Chang, A. Britz, X. Zhang, M.-F. Lin, A. Krishnamoorthy, T. Linker, D. Fritz, D. M. Neumark, R. K. Kalia, A. Nakano, P. Ajayan, P. Vashishta, U. Bergmann, S. R. Leone, Simultaneous observation of carrier-specific redistribution and coherent lattice dynamics in 2H-$MoTe_2$ with femtosecond core-level spectroscopy. *arXiv:2009.00721* (2020).
[49]Y. M. Dai, J. Bowlan, H. Li, H. Miao, S. F. Wu, W. D. Kong, Y. G. Shi, S. A. Trugman, J.-X. Zhu, H. Ding, A. J. Taylor, D. A. Yarotski, R. P. Prasankumar, Ultrafast carrier dynamics in the large-magnetoresistance material WTe_2. *Phys. Rev. B* **92**, 161104(R) (2015).
[50]C. P. Weber, *et al.*, Similar ultrafast dynamics of several dissimilar Dirac and Weyl semimetals. *J. Appl. Phys.* **122**, 223102 (2017).
[51]Y. M. Dai, B. Shen, L. X. Zhao, B. Xu, Y. K. Luo, A. P. Chen, R. Yang, X. G. Qiu, G. F. Chen, N. Ni, S. A. Trugman, J. X. Zhu, A. J. Taylor, D. A. Yarotski, R. P. Prasankumar, *2017 Conference on Lasers and Electro-Optics (CLEO)* (2017), pp. 1–2.
[52]Q. Wu, F. Sun, Q. Zhang, L. X. Zhao, G.-F. Chen, J. Zhao, Quasiparticle dynamics and electron-phonon coupling in Weyl semimetal TaAs. *Phys. Rev. Materials* **4**, 064201 (2020).
[53]M. V. Lebedev, O. V. Misochko, T. Dekorsy, N. Georgiev, On the nature of "coherent artifact". *Journal of Experimental and Theoretical Physics* **100**, 272–282 (2005).
[54]T. Winzer, A. Knorr, E. Malic, Carrier multiplication in graphene. *Nano Letters* **10**, 4839-4843 (2010).
[55]I. Gierz, M. Mitrano, J. C. Petersen, C. Cacho, I. C. E. Turcu, E. Springate, A. Söthr, A. Köhler, U. Starke, A. Cavalleri, Population inversion in monolayer and bilayer graphene. *J. Phys.: Cond. Mat.* **27**, 164204 (2015).
[56]A. N. Afanasiev, A. A. Greshnov, D. Svintsov, Relativistic suppression of Auger recombination in Weyl semimetals. *Phys. Rev. B* **99**, 115202 (2019).
[57]A. N. Afanasiev, private communication.
[58]Y. M. Sheu, Y. J. Chien, C. Uher, S. Fahy, D. A. Reis, Free-carrier relaxation and lattice heating in photoexcited bismuth. *Phys. Rev. B* **87**, 075429 (2013).
[59]J. Hohlfeld, S.-S. Wellershoff, J. Güdde, U. Conrad, V. Jähnke, E. Matthias, Electron and lattice dynamics following optical

excitation of metals. *Chem. Phys.* **251**, 237-258 (2000).
[60]W. Pötz, P. Kocevar, Electronic power transfer in pulsed laser excitation of polar semiconductors. *Phys. Rev. B* **28**, 7040–7047 (1983).
[61]X. Zhang, H.-Y. Song, X. C. Nie, S.-B. Liu, Y. Wang, C.-Y. Jiang, S.-Z. Zhao, G. Chen, J.-Q. Meng, Y.-X. Duan, H. Y. Liu, Ultrafast hot carrier dynamics of $ZrTe_5$ from time-resolved optical reflectivity. *Phys. Rev. B* **99**, 125141 (2019).
[62]K. R. O'Neal, L. M. T. Mix, M. C. Lee, B. Kuthanazhi, N. H. Jo, S. Bud'ko, P. Canfield, R. P. Prasankumar, D. A. Yarotski, *2020 Conference on Lasers and Electro-Optics (CLEO)* (2020), pp. 1–2.
[63]B. Peng, H. Zhang, W. Chen, B. Hou, Z.-J. Qiu, H. Shao, H. Zhu, B. Monserrat, D. Fu, H. Weng, C. M. Soukoulis, Subpicosecond photo-induced displacive phase transition in two-dimensional $MoTe_2$. *npj 2D Materials and Applications* **4**, 14 (2020).
[64]Z. Ni, B. Xu, M. A. Sanchez-Martinez, Y. Zhang, K. Manna, C. Bernhard, J. W. F. Venderbos, F. de Juan, C. Felser, A. G. Grushin, L. Wu, Linear and nonlinear optical responses in the chiral multifold semimetal RhSi. *arXiv:2005.13473v1* (2020).
[65]Q. Ma, S.-Y. Xu, C.-K. Chan, C.-L. Zhang, G. Chang, Y. Lin, W. Xie, T. Palacios, H. Lin, S. Jia, P. A. Lee, P. Jarillo-Herrero, N. Gedik, Direct optical detection of Weyl fermion chirality in a topological semimetal. *Nature Physics* **13**, 842–847 (2017).
[66]D. Rees, K. Manna, B. Lu, T. Morimoto, H. Borrmann, C. Felser, J. E. Moore, D. H. Torchinsky, J. Orenstein, Helicity-dependent photocurrents in the chiral Weyl semimetal RhSi. *Science Advances* **6** (2020).
[67]J. E. Moore, Optical properties of Weyl semimetals. *National Science Review* **6**, 206-208 (2018).
[68]Strictly, the time-derivative of the current.
[69]At the 2019 APS March Meeting, making reference to the 1985 film *Mad Max Beyond Thunderdome*.
[70]Y. Gao, S. Kaushik, E. J. Philip, Z. Li, Y. Qin, Y. P. Liu, W. L. Zhang, Y. L. Su, X. Chen, H. Weng, D. E. Kharzeev, M. K. Liu, J. Qi, Chiral terahertz wave emission from the Weyl semimetal TaAs. *Nature Communications* **11**, 720 (2020).
[71]Z. Ji, W. Liu, S. Krylyuk, X. Fan, Z. Zhang, A. Pan, L. Feng, A. Davydov, R. Agarwal, Photocurrent detection of the orbital angular momentum of light. *Science* **368**, 763–767 (2020).
[72]F. de Juan, A. G. Grushin, T. Morimoto, J. E. Moore, Quantized circular photogalvanic effect in Weyl semimetals. *Nature Communications* **8**, 15995 (2017).
[73]Z. Li, Y.-Q. Jin, T. Tohyama, T. Iitaka, J.-X. Zhang, H. Su, Second harmonic generation in the Weyl semimetal TaAs from a quantum kinetic equation. *Phys. Rev. B* **97**, 085201 (2018).
[74]J. Ahn, N. Nagaosa, Low-frequency divergence and quantum geometry of the bulk photovoltaic effect in topological semimetals. *arXiv:2006.06709v1* (2020).
[75]A. Avdoshkin, V. Kozii, J. E. Moore, Interactions remove the quantization of the chiral photocurrent at Weyl points. *Phys. Rev. Lett.* **124**, 196603 (2020).
[76]S. Patankar, L. Wu, B. Lu, M. Rai, J. D. Tran, T. Morimoto, D. Parker, A. Grushin, N. L. Nair, J. G. Analytis, J. E. Moore, J. Orenstein, D. H. Torchinsky, Resonance-enhanced optical nonlinearity in the Weyl semimetal TaAs. *arXiv:1804.06973* (2018).
[77]Z. Ni, K. Wang, Y. Zhang, O. Pozo, B. Xu, X. Han, K. Manna, J. Paglione, C. Felser, F. Grushin, A. G.and de Juan, E. J. Mele, L. Wu, Giant topological longitudinal circular photo-galvanic effect in the chiral multifold semimetal CoSi. *arXiv:2006.09612v2* (2020).
[78]L. Wu, S. Patankar, T. Morimoto, N. L. Nair, E. Thewalt, A. Little, J. G. Analytis, J. E. Moore, J. Orenstein, Giant anisotropic nonlinear optical response in transition metal monopnictide Weyl semimetals. *Nature Physics* **13**, 350–355 (2017).
[79]N. Sirica, *et al.*, Tracking ultrafast photocurrents in the Weyl semimetal TaAs using THz emission spectroscopy. *Phys. Rev. Lett.* **122**, 197401 (2019).
[80]N. Sirica, *et al.*, Photocurrent-driven transient symmetry breaking in the Weyl semimetal TaAs. *arXiv:2005.10308v3* (2020).
[81]K. Takasan, T. Morimoto, J. W. Orenstein, J. E. Moore, Current-induced second harmonic generation in inversion-symmetric Dirac and Weyl semimetals. *arXiv:2007.08887v1* (2020).
[82]E. J. Sie, *et al.*, An ultrafast symmetry switch in a Weyl semimetal. *Nature* **565**, 61–66 (2019).
[83]M. Y. Zhang, Z. X. Wang, Y. N. Li, L. Y. Shi, D. Wu, T. Lin, S. J. Zhang, Y. Q. Liu, Q. M. Liu, J. Wang, T. Dong, N. L. Wang, Light-induced subpicosecond lattice symmetry switch in $MoTe_2$. *Phys. Rev. X* **9**, 021036 (2019).
[84]X. Qian, J. Liu, L. Fu, J. Li, Quantum spin Hall effect in two-dimensional transition metal dichalcogenides. *Science* **346**, 1344–1347 (2014).
[85]F. Mahmood, C.-K. Chan, Z. Alpichshev, D. Gardner, Y. Lee, P. A. Lee, N. Gedik, Selective scattering between Floquet-Bloch and Volkov states in a topological insulator. *Nature Physics* **12**, 306–310 (2016).
[86]J. W. McIver, B. Schulte, F. U. Stein, T. Matsuyama, G. Jotzu, G. Meier, A. Cavalleri, Light-induced anomalous Hall effect in graphene. *Nature Physics* **16**, 38–41 (2020).
[87]U. De Giovannini, H. Hübener, Floquet analysis of excitations in materials. *Journal of Physics: Materials* **3**, 012001 (2019).
[88]T. Oka, H. Aoki, Photovoltaic Hall effect in graphene. *Phys. Rev. B* **79**, 081406 (2009).
[89]N. H. Lindner, G. Refael, V. Galitski, Floquet topological insulator in semiconductor quantum wells. *Nature Physics* **7**, 490–495 (2011).
[90]Y. H. Wang, H. Steinberg, P. Jarillo-Herrero, N. Gedik, Observation of Floquet-Bloch states on the surface of a topological insulator. *Science* **342**, 453 (2013).
[91]G. Jotzu, M. Messer, R. Desbuquois, M. Lebrat, T. Uehlinger, D. Greif, T. Esslinger, Experimental realization of the topological Haldane model with ultracold fermions. *Nature* **515**, 237–240 (2014).
[92]M. C. Rechtsman, J. M. Zeuner, Y. Plotnik, Y. Lumer, D. Podolsky, F. Dreisow, S. Nolte, M. Segev, A. Szameit, Photonic Floquet topological insulators. *Nature* **496**, 196–200 (2013).
[93]A. Narayan, Floquet dynamics in two-dimensional semi-Dirac semimetals and three-dimensional Dirac semimetals. *Phys. Rev. B* **91**, 205445 (2015).
[94]R. Wang, B. Wang, R. Shen, L. Sheng, D. Y. Xing, Floquet Weyl semimetal induced by off-resonant light. *EPL (Europhys. Lett.)* **105**, 17004 (2014).
[95]T. Kitagawa, T. Oka, A. Brataas, L. Fu, E. Demler, Transport properties of nonequilibrium systems under the application of light: Photoinduced quantum hall insulators without landau levels. *Phys. Rev. B* **84**, 235108 (2011).
[96]F. Schmitt, P. S. Kirchmann, U. Bovensiepen, R. G. Moore, L. Rettig, M. Krenz, J.-H. Chu, N. Ru, L. Perfetti, D. H. Lu, M. Wolf, I. R. Fisher, Z.-X. Shen, Transient electronic structure and melting of a charge density wave in $TbTe_3$. *Science* **321**, 1649–1652 (2008).
[97]S. Gerber, *et al.*, Femtosecond electron-phonon lock-in by photoemission and x-ray free-electron laser. *Science* **357**, 71–75 (2017).
[98]J. Kim, S.-H. Jhi, Topological phase transitions in group IV-VI semiconductors by phonons. *Phys. Rev. B* **92**, 125142 (2015).
[99]P. Hein, S. Jauernik, H. Erk, L. Yang, Y. Qi, Y. Sun, C. Felser, M. Bauer, Mode-resolved reciprocal space mapping of electron-phonon interaction in the Weyl semimetal candidate *Td*-WTe_2. *Nature Communications* **11**, 2613 (2020).
[100]A. S. Disa, M. Fechner, T. F. Nova, B. Liu, M. Först, D. Prabhakaran, P. G. Radaelli, A. Cavalleri, Polarizing an antiferromagnet by optical engineering of the crystal field. *Nature Physics* **16**, 937–941 (2020).

[101]M. Först, C. Manzoni, S. Kaiser, Y. Tomioka, Y. Tokura, R. Merlin, A. Cavalleri, Nonlinear phononics as an ultrafast route to lattice control. *Nature Physics* **7**, 854 (2011).
[102]H. J. Zeiger, J. Vidal, T. K. Cheng, E. P. Ippen, G. Dresselhaus, M. S. Dresselhaus, Theory for displacive excitation of coherent phonons. *Phys. Rev. B* **45**, 768 (1992).
[103]C. P. Weber, M. G. Masten, T. C. Ogloza, B. S. Berggren, M. K. L. Man, K. M. Dani, J. Liu, Z. Mao, D. D. Klug, A. A. Adeleke, Y. Yao, Using coherent phonons for ultrafast control of the Dirac node of $SrMnSb_2$. *Phys. Rev. B* **98**, 155115 (2018).
[104]B. He, C. Zhang, W. Zhu, Y. Li, S. Liu, X. Zhu, X. Wu, X. Wang, H.-H. Wen, M. Xiao, Coherent optical phonon oscillation and possible electronic softening in WTe_2 crystals. *Sci. Rep.* **6**, 30487 (2016).
[105]Or perhaps the $1T'$ structure, which is also centrosymmetric and precludes Weyl points.
[106]H.-J. Kim, S.-H. Kang, I. Hamada, Y.-W. Son, Origins of the structural phase transitions in $MoTe_2$ and WTe_2. *Phys. Rev. B* **95**, 180101 (2017).
[107]B. Xu, L. X. Zhao, P. Marsik, E. Sheveleva, F. Lyzwa, Y. M. Dai, G. F. Chen, X. G. Qiu, C. Bernhard, Temperature-driven topological phase transition and intermediate Dirac semimetal phase in $ZrTe_5$. *Phys. Rev. Lett.* **121**, 187401 (2018).
[108]B. Monserrat, A. Narayan, Unraveling the topology of $ZrTe_5$ by changing temperature. *Phys. Rev. Research* **1**, 033181 (2019).
[109]N. Aryal, X. Jin, Q. Li, A. M. Tsvelik, W. Yin, Topological phase transition and phonon-space Dirac topology surfaces in $ZrTe_5$. *arXiv:2004.13326v1* (2020).
[110]C. Vaswani, *et al.*, Light-driven raman coherence as a nonthermal route to ultrafast topology switching in a Dirac semimetal. *Phys. Rev. X* **10**, 021013 (2020).
[111]T. Konstantinova, L. Wu, W.-G. Yin, J. Tao, G. D. Gu, X. J. Wang, J. Yang, I. A. Zaliznyak, Y. Zhu, Photoinduced Dirac semimetal in $ZrTe_5$. *arXiv:2010.04285* (2020).
[112]L. L. Wang, Expansive open Fermi arcs and connectivity changes induced by infrared phonons in $ZrTe_5$. *arXiv:2004.13330* (2020).
[113]G. E. Topp, N. Tancogne-Dejean, A. F. Kemper, A. Rubio, M. A. Sentef, All-optical nonequilibrium pathway to stabilising magnetic Weyl semimetals in pyrochlore iridates. *Nature Communications* **9**, 4452 (2018).
[114]D. Soranzio, M. Peressi, R. J. Cava, F. Parmigiani, F. Cilento, Ultrafast broadband optical spectroscopy for quantifying subpicometric coherent atomic displacements in WTe_2. *Phys. Rev. Research* **1**, 032033 (2019).
[115]K. Sokolowski-Tinten, C. Blome, J. Blums, A. Cavalleri, C. Dietrich, A. Tarasevitch, I. Uschmann, E. Förster, M. Kammler, M. Horn-von Hoegen, D. von der Linde, Femtosecond X-ray measurement of coherent lattice vibrations near the Lindemann stability limit. *Nature* **422**, 287 (2003).
[116]D. M. Juraschek, S. F. Maehrlein, Sum-frequency ionic Raman scattering. *Phys. Rev. B* **97**, 174302 (2018).
[117]R. Mankowsky, *et al.*, Nonlinear lattice dynamics as a basis for enhanced superconductivity in $YBa_2Cu_3O_{6.5}$. *Nature* **516**, 71–73 (2014).
[118]M. Mitrano, A. Cantaluppi, D. Nicoletti, S. Kaiser, A. Perucchi, S. Lupi, P. Di Pietro, D. Pontiroli, M. Riccò, S. R. Clark, D. Jaksch, A. Cavalleri, Possible light-induced superconductivity in K_3C_{60} at high temperature. *Nature* **530**, 461–464 (2016).
[119]X. Li, T. Qiu, J. Zhang, E. Baldini, J. Lu, A. M. Rappe, K. A. Nelson, Terahertz field–induced ferroelectricity in quantum paraelectric $SrTiO_3$. *Science* **364**, 1079–1082 (2019).
[120]D. M. Juraschek, P. Narang, Giant phonon-induced effective magnetic fields in $4f$ paramagnets. *arXiv:2007.10556* (2020).
[121]In my own work, ZrSiS and NbAs showed no damage after many hours of mid-infrared excitation at 1 kHz and 10 mJ/cm^2.
[122]S. Mizukami, A. Sugihara, S. Iihama, Y. Sasaki, K. Z. Suzuki, T. Miyazaki, Laser-induced THz magnetization precession for a tetragonal Heusler-like nearly compensated ferrimagnet. *Applied Physics Letters* **108**, 012404 (2016).
[123]S. Solopow, Wavelength dependent demagnetization dynamics in Co_2MnGa Heusler-alloy, doctoral thesis, Universität Potsdam (2019).
[124]D. Cheskis, Magneto-optical tools to study effects in Dirac and Weyl semimetals. *Symmetry* **12**, 1412 (2020).
[125]E. Ott, "Caos in dynamical systems," (Cambridge University Press, New York, 1994).
[126]H. Hentschel and I. Procaccia, "The infinite number of generalized dimensions of fractals and strange attractors," Physica D **8**, 435–444 (1983).
[127]P. Grassberger, "Generalized dimensions of strange attractors," Physica Lett. A **97**, 227–230 (1983).
[128]T. Halsey, M. Jensen, L. Kadanoff, I. Procaccia, and B. Shraiman, "Fractal measures and their singularities: the characterization of strange sets," Phys. Rev. A **33**, 1141–1151 (1986).
[129]A. Chhabra and R. Jensen, "Direct determination of the f(α) singularity spectrum," Phys. Rev. Lett. **62**, 1327–1330 (1989).
[130]A. Chhabra, C. Meneveau, R. Jensen, and K. Sreenivasan, "Direct determination of the f(α) singularity spectrum and its application to fully developed turbulence," Phys. Rev. A **40**, 5284–5295 (1989).
[131]J. T.A. Witten and L. Sander, "Diffusion-limited aggregation, a kinetic critical phenomenon," Phys. Rev. Lett. **47**, 1400–1403 (1981).
[132]L. M. Sander, "Diffusion-limited aggregation, a kinetic critical phenomenon?" Contemp. Phys. **41**, 203–218 (2000).
[133]A. Chaudhari, C.-C. S. Yan, , and S.-L. Lee, "Multifractal scaling analysis of autopoisoning reactions over a rough surface," J. Phys. A: Math. Gen. **36**, 3757–3772 (2003).
[134]D. Adams, L. M. Sander, E. Somfai, and R. M. Ziff, "The harmonic measure of diffusion-limited aggregates including rare events," EPL. **87**, 20001 (2009).
[135]Y. Kamer, G. Ouillon, and D. Sornette, "Barycentric fixed-mass method for multifractal analysis," Phys. Rev. E **88**, 02292 (2013).
[136]P. Jizba and T. Arimitsu, "The world according to rényi: thermodynamics of multifractal systems," Ann. Phs-New York **312**, 17–59 (2004).
[137]R. Vavrek, L. G. Balázs, A. Mészáros, I. Horváth, and Z. Bagoly, "Testing the randomness in the sky-distribution of gamma-ray bursts," Mon. Not. R. Astron. Soc. **391**, 741–748 (2008).
[138]P. Sarkar, J. Yadav, B. Pandey, and S. Bharadwaj, "The scale of homogeneity of the galaxy distribution in sdss dr6," Mon. Not. R. Astron. Soc. **399**, L128–L131 (2009).
[139]B. N. Miller and J.-L. Rouet, "Cosmology in one dimension: fractal geometry, power spectra and correlation," J. Stat. Mech. , P12028 (2010).
[140]J. K. Yadav, J. S. Bagla, and N. Khandai, "Fractal dimension as a measure of the scale of homogeneity," Mon. Not. R. Astron. Soc. **405**, 2009–2015 (2010).
[141]J. Gaite, "The fractal geometry of the cosmic web and its formation," Adv. Astron. , 6587138 (2019).
[142]E. Fernández, J. Bolea, G. Ortega, and E. Louis, "Are neurons multifractals?" J. Neurosci. Methods. **89**, 151–157 (1999).
[143]Y. Zheng, J. Gao, J. C. Sanchez, J. C. Principe, and M. S. Okun, "Multiplicative multifractal modeling and discrimination of human neuronal activity," Phys. Lett. A **344**, 253–264 (2005).
[144]J. G. Milton, "Introduction to focus issue: bipedal locomotion - from robots to humans," Chaos **19**, 253–264 (2009).
[145]R. Uthayakumar and D. Easwaramoorthy, "Multifractal-wavelet based denoising in the classification of healthy and epileptic eeg signals," Fluct Noise Lett **11**, 1250034 (2012).
[146]T. Zorick and M. A. Mandelkern, "Multifractal detrended fluctuation analysis of human eeg: preliminary investigation and comparison with the wavelet transform modulus maxima technique," PLoS One **8**, e68360 (2013).
[147]G. Vergotte, S. Perrey, M. Muthuraman, S. Janaqi, and K. Torre, "Concurrent changes of brain functional connectiv-

ity and motor variability when adapting to task constraints," Front. Physiol. **9**, 909 (2018).
[148]L. G. S. França, J. G. V. Miranda, M. Leite, N. K. Sharma, M. C. Walker, L. Lemieux, and Y. Wang, "Fractal and multifractal properties of electrographic recordings of human brain activity: toward its use as a signal feature for machine learning in clinical applications," Front. Physiol. **9**, 1767 (2018).
[149]Y. Cheng, "Defining urban and rural regions by multifctal spectrums of urbanization," Fractals **24**, 165004 (2016).
[150]B. Chakraborty, K. Haris, N. M. G. Latha, and A. Menezes, "Multifractal approach for seafloor characterization," IEEE Geosci Remote S **11**, 54–58 (2014).
[151]A. Wawrzaszek and W. M. Macek, "Observation of the multifractal spectrum in solar wind turbulence by ulysses at high latitudes," J Geophys Res-Space **115**, A07104 (2010).
[152]B. Gualtiero and D. Domeisen, "Nonlinear stratospheric variability: multifractal de-trended fluctuation analysis and singularity spectra," Proc. R. Soc. A. **472**, 2191 (2016).
[153]E. Pardo-Igúzquiza and P. A. Dowd, "Fractal analysis of karst landscapes," Math. Geosci. **52**, 543–563 (2019).
[154]R. Dickman, "Rain, power laws, and advection," Phys. Rev. Lett. **90**, 108701 (2003).
[155]R. Dickman, "Fractal rain distributions and chaotic advection," Braz. Jour. Phy. **34**, 337–346 (2004).
[156]O. Peters, C. Hertlein, and K. Christensen, "A complexity view of rainfall," Phys. Rev. Lett. **88**, 018701 (2001).
[157]O. Peters and K. Christensen, "Rain: relaxations in the sky," Phys. Rev. E **66**, 036120 (2002).
[158]P. Holmes and E. C. Zeeman, "A nonlinear oscillator with a strange attractor," Philos. Trans. Roy. Soc. London Ser. A **292**, 419–448 (1979).
[159]M. Hénon, "A two-dimensional mapping with a strange attractor," Commun. Math. Phys. **50**, 69–77 (1976).
[160]K. Ikeda, "Multiple-valued stationary state and its instability of the transmitted light by a ring cavity system," Opt. Commun. **30**, 257–261 (1979).
[161]K. Ikeda, H. Daido, and O. Akimoto, "Optical turbulence: chaotic behavior of transmitted light from a ring cavity," Phys. Rev. Lett **45**, 709–712 (1980).
[162]R. Lozi, "Un attracteur étrange (?) du type attracteur de hnon," J. Phys. Colloques **39**, 9–10 (1978).
[163]H. Nusse and J. Yorke, "Dynamics: Numerical explorations," (Springer, New York, 1994).
[164]J. Sprott and A. Xiong, "Classifying and quantifying basins of attraction," Chaos **25**, 083101 (2015).
[165]N. Fiedler-Ferrara and C. P. C. do Prado, "Caos uma introdu," (Editora Edgar Blücher Ltd, São Paulo, 1994) Chap. 3, p. 300.
[166]V. I. Arnol'd, "Small denominators I: on the maps of circumference on itself," Trans. Am. Math. Soc. **46**, 213–284 (1965).
[167]Y. G. Sinai, "Gibbs measures in ergodic theory," Russ. Math. Surv. **27**, 21–69 (1972).
[168]R. M. May, "Simple mathematical models with very complicated dynamics," Nature **261**, 459–467 (1976).
[169]G. Zaslavsky, "The simplest case of a strange attractor," Phys. Lett. A **69**, 145–147 (1978).
[170]G. Zaslavsky and R. Kh.-R.Ya, "Singularities of transition to a turbulent motion," Sov. Phys. JETP **49**, 1039–1044 (1979).
[171]"Zaslavskii map," Wikipedia https://en.wikipedia.org/wiki/Zaslavskii_map (2020).
[172]G. Duffing, "Erzwungene schwingungen bei veränderlicher eigenfrequenz und ihre technische bedeutung," (F. Braunschweig, F. Vieweg & Sohn, 1918).
[173]F. C. Moon and P. J. Holmes, "A magnetoelastic strange attractor," J. Sound Vib. **65**, 275–296 (1979).
[174]E. Lorenz, "Deterministic nonperiodic flow," J. Atmos. Sci. **20**, 130–141 (1963).
[175]O. Rössler, "An equation for continuous chaos," Phys. Lett. A **57**, 397–398 (1976).
[176]T. Matsumoto, "A chaotic attractor from chua's circuit," IEEE Trans. Circuits Syst. I, Reg. Papers **12**, 1055–1058 (1984)